Light Metals 2014
Edited by: John Grandfield
TMS (The Minerals, Metals & Materials Society), 2014

A MODELLING OF HEAT LOSSES IN ALUMINIUM REDUCTION CELL WITH SLOTTED ANODES

YANG Shuai, LI Jie, XU Yujie, ZHANG Hongliang, LV Xiaojun, JIA Ming

School of Metallurgy and Environment, Central South University, Changsha, Hunan, 410083, P.R. China

Keywords: Aluminum reduction cell; Heat transfer coefficient; Heat losses; CFD; Slotted anode

Abstract

The heat losses of aluminium reduction cells depend strongly on the heat transfer coefficients between the bath and side ledge or anodes. Using of anodes with slots can greatly change heat transfer. In order to investigate the heat loss dynamics in reduction cells with slotted anodes, a modeling of heat transfer coefficients in cells was firstly undertook. This enables understanding of how slotted anode changes heat dissipation from the bath. Then, a thermal field was been calculated by using heat transfer coefficients obtained in the first step. All these studies were carried out with 500kA cells.

Introduction

Most Chinese aluminium manufacturers are facing the rising price of electric energy. For example, electric energy consumption account for more than 45% of the total production costs. In order to reduce the energy cost, some innovative methods have been put forward in some potlines, which include novel structural cathodes (NSC) and modified anodes, as well as new control algorithms[1-4]. Among these methods, slotted anode has already been widely used and proves to be energy effective.

However, some cell behavior is changed when slotted anodes are used. It is well known that there exists a thin gas layer under anodes which results in extra voltage drop and heat generation. Some studies have shown that the melt flow in aluminum reduction cells is mainly driven by gas bubbles and electromagnetic forces (EMFs)[5-6]. As the bubbles can partially be released by the grooves, a more gentle circulation of electrolyte would be observed when flat bottom anodes are replaced by slotted anodes. And heat transfer dynamics is changed too as it is related to the melt flow.

Owing to the complex relation between slotted anodes and heat loss, it becomes the focus of the computational studies of the cell thermal status. However, most of the studies have not paid enough attention to the heat losses of slotted anodes. Therefore, there is no explanation about whether additional thermal insulation is needed or not with slotted anodes.

This paper firstly introduces a CFD model for the flow and heat transfer coefficients in a 500kA pre-baked anode cell based on the commercial code CFX, in which the effect of EMFs and bubbles were studied. Then, the results from cells with flat bottom anodes and with slotted anodes were compared for examining characters of heat convection from bath and around. At last, two slices of a FEM (finite element method) model were built to explore heat transfer status based on data from CFD models.

Heat transfer coefficients

Flow model

It is clear that bubbles and EMFs were the two major factors in driving the bath flow inside the cell cavity. Previous studies showed that bubble driven flow was the dominant part of the bath flow inside the channels[7-8]. Thus, Severo et al[9] calculated bath-ledge heat transfer coefficients in a 164kA cell in which EMFs was not included. However, the recent research have made it clear that EMFs should be taken into account in flow field calculation[6]. Therefore, a CFD model was developed by taking into account the bubbles and EMFs driven flow in a full scale model of the cell, where the inhomogeneous equations for conservation of mass and momentum can be written as follows:

$$\frac{\partial}{\partial t}(r_\alpha \rho_\alpha) + \nabla \cdot (r_\alpha \rho_\alpha U_\alpha) = 0 \tag{1}$$

$$\begin{aligned} &\frac{\partial}{\partial t}(r_\alpha \rho_\alpha U_\alpha) + \nabla \cdot (r_\alpha (\rho_\alpha U_\alpha \times U_\alpha)) \\ &= -r_\alpha \nabla p_\alpha + \nabla \cdot (r_\alpha \mu_{\alpha eff} (\nabla U_\alpha + (\nabla U_\alpha)^T)) \\ &\quad + S_{M\alpha} + M_\alpha \end{aligned} \tag{2}$$

where r_α, ρ_α, U_α, P_α and $\mu_{\alpha eff}$ are volume fraction, density, velocity, pressure and effective viscosity of phase α respectively.

The EMFs were treated as the momentum source term $S_{M\alpha}$ all over the bath domain, which could be calculated from the cross product of electric current density and magnetic induction intensity. For the interfacial forces M_α, only the interphase drag force induced by gas bubble was considered. The effect of metal pad movement was neglected for the complex existence of a liquid bath film between liquid metal and solidified ledge[10].

For the heat transferring in bath, most of it is Joule heat generated by the ohmic effect, only a very small part can be attributed to friction and other mechanical

motions. When those mechanical heat sources are neglected, the energy equation can be written as follows:

$$\frac{\partial}{\partial t}(\rho C_p T) + \nabla \cdot (\rho U C_p T) = \nabla \cdot (\lambda \nabla T + \frac{\mu_T}{\sigma_T} \nabla T) + Q \quad (3)$$

Where T、C_p、λ、μ_T and σ_T are temperature, fluid heat capacity, heat conductivity coefficient, turbulence viscosity and turbulence Prandtl number. Q is heat source of the fluid.

Wall functions

Heat transfer between bath and ledge can be described by Newton's law of cooling, which has the following form:

$$q_b = h_b (T_w - T_f) \quad (4)$$

With the wall functions used in the CFX code, the dimensionless temperature near the wall can be written as:

$$T^+ = \frac{\rho C_p u_\tau (T_w - T_f)}{q_b} \quad (5)$$

So, the heat transfer coefficients h_b can be calculated with the wall function in the equation (6).

$$h_b = \frac{\rho C_p u_\tau}{T^+} \quad (6)$$

With the help of turbulence model and the thermal law-of-the-wall function of B.A. Kader[11], u_τ and T^+ can be calculated using the follow equations:

$$u^+ = \frac{U_t}{u_\tau} = \frac{1}{\kappa} \ln(y^+) + C \quad (7)$$

$$T^+ = 2.12 \ln(y^+) + \beta \quad (8)$$

$$\beta = (3.85 Pr^{1/3} - 1.3)^2 + 2.12 \ln(Pr) \quad (9)$$

where T_w is the temperature at the wall; T_f is the near-wall fluid temperature; Pr is the fluid Prandtl number; u^+ is the dimensionless velocity near the wall relative to skin friction velocity u_τ; y^+ is the dimensionless position with respect to the boundary layer thickness; C is a constant related to wall. C is a log-layer constant depending on wall roughness. U_t is the known velocity tangent to the wall.

Application Model

As the analysis above, heat transfer coefficients are functions of the liquids properties and fluid flow characteristics, which are the focus of the modeling. Since the heat transfer coefficient is unrelated to the temperature at the wall and the near-wall fluid temperature, two fixed temperatures were used respectively for T_w and T_f . In addition, the side effect of gas coverage on heat transfer is taken into consideration. Then, a geometry of full scale bath in a 500 kA cell was included when taking the effect of asymmetry flow pattern into account. The rate of gas generation for the case of unslotted anodes are of 5.01×10^{-2} kg/m²s and 8.83×10^{-3} kg/m²s respectively at the anodes bottom and anodes sides for a cell working with current density of 0.83A/cm² and CE of 92%, based on literature [6]. The model has 48 anodes and its size is 1800 mm x 740 mm x 600 mm. The sidewall channels are 290 mm wide; inter-anode channels width is equal to 40 mm; central channels width is equal to 180 mm; anode to cathode distance (ACD) is 42 mm and all anodes are immersed 178 mm in the bath.

Results and discussion

Driven factors examination

The local heat transfer coefficients are showed as Fig. 1. It is obvious that the heat transfer coefficient changes greatly with variation of location. The maximal value is about 2947 $W \cdot m^{-2} \cdot K^{-1}$, but there is a very small area of the coefficient exceeding 2000 $W \cdot m^{-2} \cdot K^{-1}$. Particularly, it is clear to observe that the bath-ledge heat transfer coefficients on long side are between 1300 $W \cdot m^{-2} \cdot K^{-1}$ and 1900 $W \cdot m^{-2} \cdot K^{-1}$ as partially shown on Fig. 2. However, the range of the coefficients is larger for end sides where the coefficients on many points are more than 2000 $W \cdot m^{-2} \cdot K^{-1}$, as Fig. 3 shows. And on the anodes bottom surface, a relatively small heat transfer coefficients between bath and anodes would be obtained because of the existence of gas layer which will be discussed in the slotted anodes case.

In order to investigate the effect of gas bubbles and EMFs on the heat transfer coefficients between bath and side ledge and between bath and anode, contrastive studies are made where the bath melt is driven by different kinds of forces, i.e. anode gas only, EMFs only and both of the two forces. The average values under different affecting factors are shown in Table 1.

Table 1 Average values of the heat transfer coefficient under different effects

Effector factor	Bath-anode /$W \cdot m^{-2} \cdot K^{-1}$	Bath-sideledge (cell side) /$W \cdot m^{-2} \cdot K^{-1}$	Bath-sideledge (cell end) /$W \cdot m^{-2} \cdot K^{-1}$
EMFs only	501	696	654
Anode gas only	482	1370	1650
Both anode gas and EMFs	478	1473	1894

The data in table 1 explains that both gas bubbles and EMFs have some influences on heat transfer coefficients and their combined action will enhance the heat transfer between bath and ledge. However, their heat dissipation characteristics are very different on the anode bottom surface. In particular, the averaged heat transfer coefficient obtained was 1473 $W \cdot m^{-2} \cdot K^{-1}$ for bath-ledge. This value is close to Severo et al[9] obtained in a 164 kA cell using CFD also which the value is 1370 $W \cdot m^{-2} \cdot K^{-1}$, but somewhat lower than the obtained using the correlations presented by Dupuis et al. which is around 2000 $W \cdot m^{-2} \cdot K^{-1}$ [12].

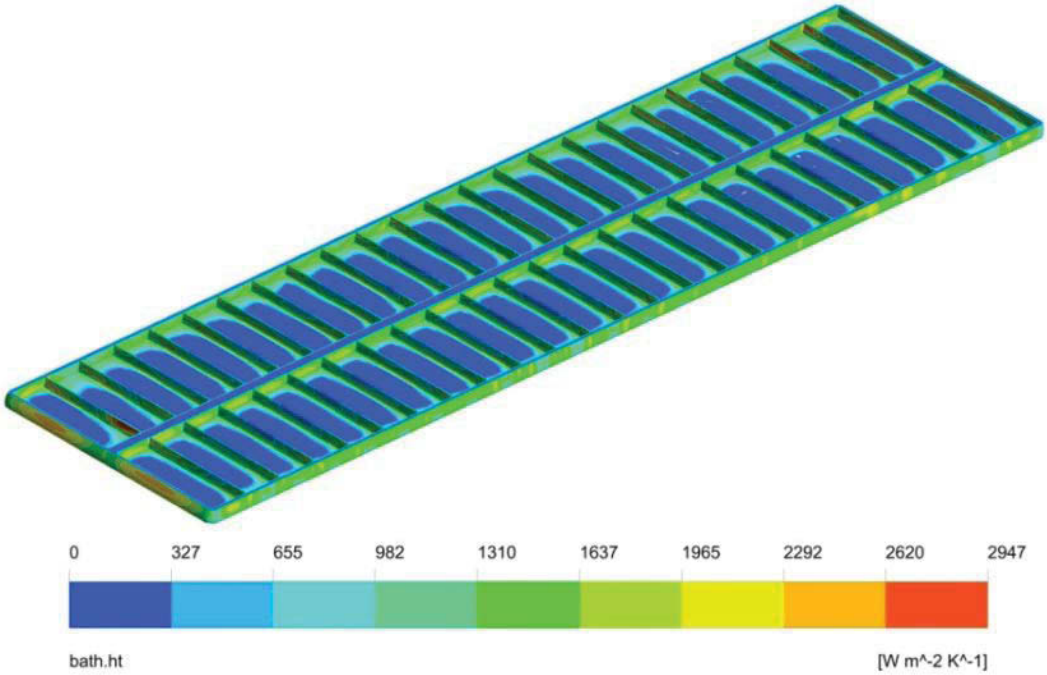

Fig. 1 Local heat transfer coefficients distribution of 500 kA

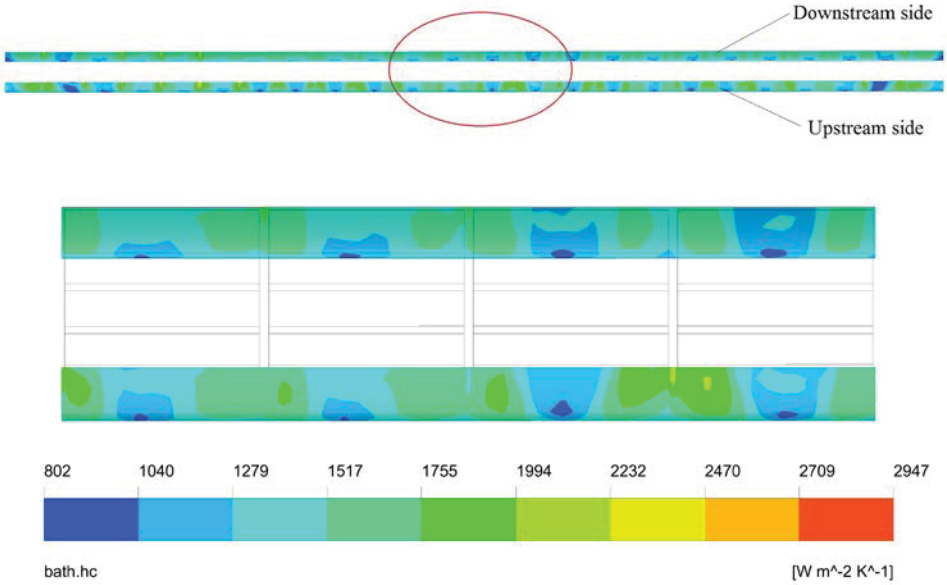

Fig. 2 Heat transfer coefficients distribution on ledge of the cell side (partial)

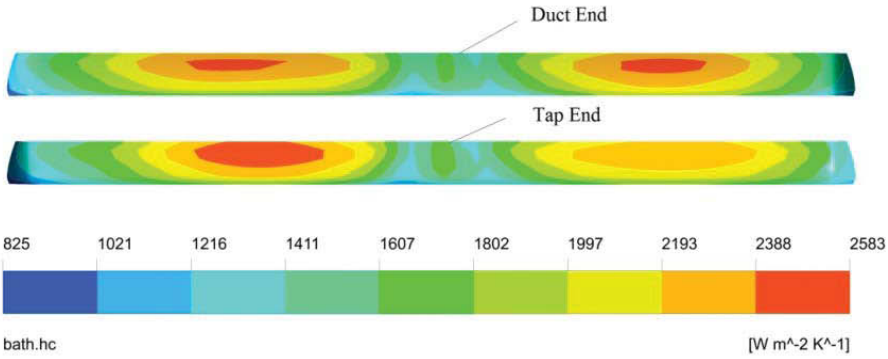

Fig. 3 Heat transfer coefficients distribution on ledge of the cell end

Slotted anodes case

As described in the model, anodes used in our 500 kA cell are really large, which are 1800 mm in length and 740 mm in width. Apparently, compare to those common anodes used in smaller cells, using of these large anodes will undoubtedly result in a thick gas layer under the bottom of anodes, which is unfavorable in the electrolysis process for its negative effects on cell performance. Thus, when putting this 500 kA cell sketch into practice, slot cutting on this large anode is needed. The authors have proved that good slot cutting arrangements could effectively reduce the gas volume below the anodes[13]. Therefore, a reduced rate of gas injection was used in the slotted anodes case for calculating heat transfer coefficients. The average values when using different kinds of anodes are shown in Table 2.

The data showed in table 2 gives information about how slot cutting changes the heat transfer coefficients in different areas. For heat transfer on side ledge, the values of coefficients decreases with the use of slotted anodes, both on the long side or end side of the cell. The extent of the decreasing is 17.04% and 20.86% respectively. However, the average heat transfer coefficients on anode bottom increase from 478 $W \cdot m^{-2} \cdot K^{-1}$ to 855 $W \cdot m^{-2} \cdot K^{-1}$ with the use of slotted anodes, about 78.87%. The following two points can explain these changes. The first one is that slot cutting on anodes have the effect of reducing average bath velocity. This is because the path of the gas to be released is shorter so the bath was less stirred, which would not be discussed in details here but the average bath velocity decreases from 0.114 $m \cdot s^{-1}$ to 0.099 $m \cdot s^{-1}$ in our cases. The second point is that gas coverage on anode bottom surface reduces significantly with the use of slotted anodes, as illustrated on Fig. 4 and Fig. 5. It is obvious that bath and anode bottom have more opportunity to get in touch with each other when slot cutting is adopted.

Table 2 Average values of the heat transfer coefficient in different cases

case	Bath-anode /$W \cdot m^{-2} \cdot K^{-1}$	Bath-sideledge (cell side) /$W \cdot m^{-2} \cdot K^{-1}$	Bath-sideledge (cell end) / $W \cdot m^{-2} \cdot K^{-1}$
Unslotted	478	1473	1894
Slotted	855	1222	1499

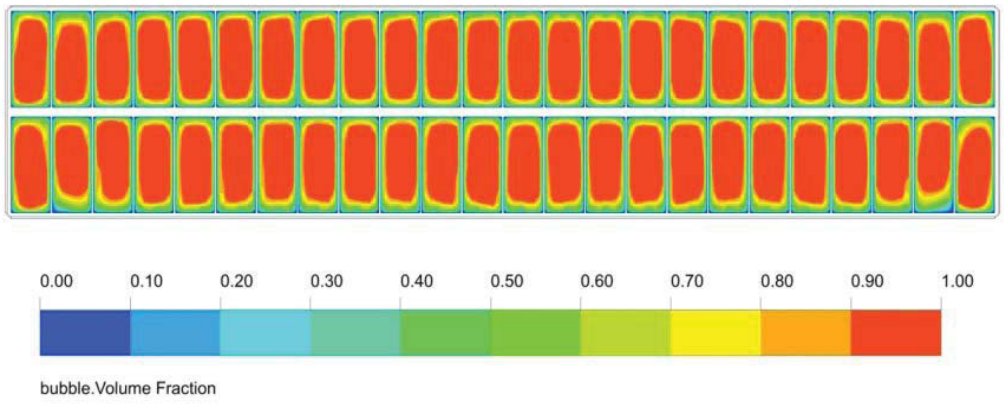

Fig. 4 Gas coverage distribution on anode bottom surface when using unslotted anode

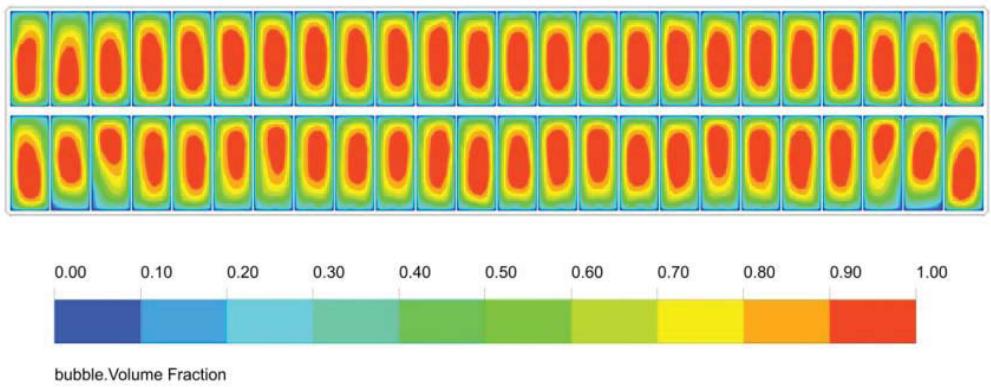

Fig. 5 Gas coverage distribution on anode bottom surface when using slotted anode

Heat Losses

After the obtainment of heat transfer coefficients, the heat losses of the cell were calculated in a FEM model. As a result of the much bigger electric resistance of the bath, a large quantity of heat is produced here. The heat transfer between bath and side ledge as well as anodes can be described as Newton's law of cooling. Then, heat contact was defined to model the heat transfer which the formula is as follows:

$$q = TCC \times \left(T_t - T_c\right) \tag{10}$$

where q is the heat flux per area, TCC is the thermal contact conductance coefficient, equal to the heat transfer coefficient. T_t and T_c are the temperatures of contacted surfaces respectively.

According to many test, slot cuttings on anodes have the benefits of about 20-30 mV total energy saving by translating the CE improvement into voltage drop[4]. Thus, the ACD used in the heat loss calculation of slotted case is 41 mm, and 1 cm thicker of cover materials was adopted in order to strengthen the thermal insulation. The results of heat losses statistics are shown in Table 3. Besides, the ledge shapes are shown in Fig. 6.

Table 3 Heat losses of the cell in different cases

Parameters	Unslotted case	Slotted case
1. Heat loss of anode	54.08%	53.55%
of which: cover materials	22.16%	20.28%
Stub and rod	31.92%	33.27%
2. Heat loss of cathode	45.92%	46.45
of which: pot shell anf cradle	36.60%	36.88
Collector bar and flexible	9.32%	9.57

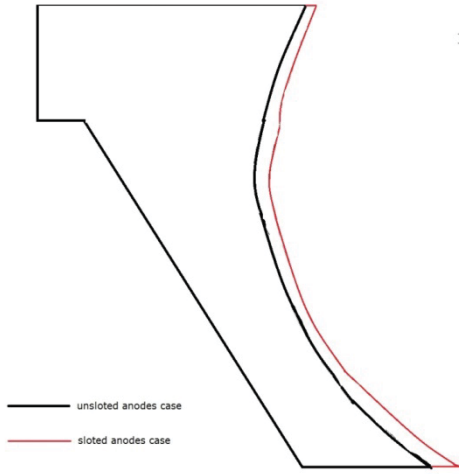

Fig. 6 Calculated ledge profiles for 500 kA cells

Table 3 shows that the difference of heat loss in the two cases is very small. With the help of adopting 1cm increase of thickness, heat loss of cover materials drops about 2%. However, heat loss from stubs increases a little because stub temperature rises due to stronger heat transfer between bath and anodes in the slotted case. Ledge shape also shows very little difference, average thickness increased about 1.5 cm, which would not affect CE and stability too much. In general, slot cuttings on anodes have little influence on heat loss of 500 kA cells, no extra thermal insulation measures is needed except for slight adjustment of cover materials thickness.

Conclusions

This paper firstly demonstrates the use of CFD method in the processing and analyzing of heat transfer coefficients between bath and side ledge and anodes in 500 kA cells. The results show that both EMFs and gas bubbles have some influences on heat transfer coefficients and their combined action will enhance the

heat transfer between bath and ledges. To the cells with slotted anodes, the average values of coefficients decrease on side ledge and increase on anode bottom. Thermal field is calculated by using the data from the CFD model. A comparison between using of slotted and unslotted anodes showed that slot cuttings on anodes have little influence on heat loss of 500 kA cells, and no extra thermal insulation measures need to be taken except for slight adjustment of cover materials thickness.

Acknowledgements

The authors are grateful for the financial support of the National Natural Science Foundation of China (51104187)、(51274241) and (51204211).

References

[1] Feng Naixiang, Tian Yingfu, Peng Jianping, et al. New Cathodes in Aluminum Reduction Cells. Light Metals 2010: 405-408

[2] LI Jie, LV Xiao-jun, ZHANG Hong-liang, LIU Ye-xiang. Development of low-voltage energy-saving aluminum reduction technology. Light Metals 2013: 557-559

[3] Yingfu Tian , Hesong Li , Longhe Wei , Xi Cao , Jianguo Yin. Industry test of perforation anode in aluminum electrolysis technology. Light Metals 2013: 567-571

[4] Meier M W, Perruchoud R C, Fischer W K. Production and performance of slotted anodes. Light Metals 2007: 293-298.

[5] Doheim M A, El-Kersh A M, Ali M M. Computational modeling of flow in aluminum reduction cells due to gas bubbles and electromagnetic forces. Metallurgical and Materials Transactions B, 2007, 38(1): 113-119

[6] LI Jie, XU Yu- jie, ZHANG Hong -liang, LAI Yan -qing. An inhomogeneous three -phase model for the flow in aluminium reduction cells. International Jour nal of Multiphase Flow, 2011, 37(1): 46 –54.

[7] Severo D S, Gusberti V, Pinto E C V, Moura R R. Modeling the Bubble Driven Flow in the Electrolyte as a Tool for Slotted Anode Design Improvemen. Light Metals 2007: 287-292.

[8] Cooksey M A, Yang W. PIV Measurements on Physical Models of Aluminium Reduction Cells. Light Metals 2006: 485-488359-365.

[9] Severo D S, Gusberti V. A modeling approach to estimate bath and metal heat transfer coefficients. Light Metals 2009: 557–562

[10] Solheim A. Towards a Proper Understanding of Sideledge Facing the Metal in Aluminum Cells? Light Metals 2006: 367-369

[11] Kader B A.Temperature and Concentration Profiles in Fully Turbulent Boundary Layers. International Journal of Heat and Mass Transfer, 1981, 24(9): 1541-1544.

[12] Dupuis M, Bojarevics V. Weakly coupled thermo-electric and MHD mathematical models of an aluminum electrolysis cell. Light Metals 2005: 449-454

[13] Yang Shuai, Zhang Hong-liang, Xu Yu-jie, et al. Effects of slot cutting at prebaked anodes on buble elimination in aluminum reduction cell .Journal of Central South University, 2012, 43(12): 4617-4625.